REVIEW

A Comprehensive Survey of Silicon Thin-film Solar Cell: Challenges and Novel Trends

Khalil ElKhamisy[1] · Hamdy Abdelhamid[2,3] · El-Sayed M. El-Rabaie[4] · Nariman Abdel-Salam[5]

Abstract

Solar cells are commonly recognized as one of the most promising devices that can be utilized to produce energy from renewable sources. As a result of their low production costs, little material consumption, and projected increasing trajectory in terms of efficiency, thin-film solar cells have emerged as the technology of choice in the solar industry at present. This study aims to provide a comprehensive review of silicon thin-film solar cells, beginning with their inception and progressing up to the most cutting-edge module made in a laboratory setting. There is a review of the fantastic development of each technology, as well as its cell configuration, restrictions, equivalent circuit model, cell performance, and global market share. The dependability and availability of cell materials, in addition to the comparison of numerous characteristics, are both areas of research that are conducted concurrently for each of the distinct technologies. New advances in solar cells are also highlighted; these hold the potential to be significant variables and solutions in the process of the future's development. This abbreviated and brief version of the comprehensive analysis is provided to readers in the hope that it will aid them in evaluating potential research avenues about the proper applications and production of solar cells.

Keywords Thin-film solar cells · Renewable energy · Cell configuration · Equivalent circuit model · The emerging solar cell technologies

Introduction

Due to rising energy demand as well as environmental and global issues associated with the widespread use of fossil fuels, scientists believe that solar energy is the most substantial and dependable renewable energy source currently available. Solar energy is also the most widely available, dependable, and cost-effective renewable energy source [1].

Organic solar cells, photovoltaic (PV) cells, and hybrid solar cells are the three types of solar cells based on the technology used or the manufacturing process. PV cells are the most common type of solar cell, followed by organic solar cells and hybrid solar cells. In a nutshell, photovoltaic cells are devices that convert solar energy into electrical energy. Approximately 89% of the global solar cell market is made up of first-generation solar cells [2, 3].

Crystalline silicon was used in the first generation of solar cells. Despite the benefits of silicon materials in PhotoVoltaics, they have a low energy conversion efficiency of 27.6% and a high manufacturing cost. To address the drawbacks of using crystalline silicon semiconductors, an alternative technology based on micron-sized solar cells was developed; however, efficiency remains low.

The third generation of solar cells is predicated on the use of new materials and technologies that have yet to be commercialized but are expected to have the highest theoretical efficiency as well as the lowest manufacturing cost. Although these new materials and technologies are not yet widely available, they act as the basis for the third generation

✉ Nariman Abdel-Salam
   nariman_abdelsalam@cic-cairo.com

1 Department of Communications and Computers Engineering, the Higher Institute of Engineering, El-Shorouk City 11837, Egypt

2 Collage of Engineering and Information Technology, Electrical Engineering Department, Ajman University, Ajman, United Arab Emirates

3 Center of Nano-Electronics and Devices (CND), Zewail City of Science and Technology, 6th October City, Giza, Egypt

4 Department of Electronics and Communications, Faculty of Electronic Engineering, Menoufia University, Menoufia, Egypt

5 Department of Electronics and Communications Engineering, Faculty of Engineering, Canadian International College (CIC), Giza, Egypt

of solar cells. Despite the numerous benefits of thin-film silicon solar cells [4], their conversion efficiency, as well as the efficiency of the processes involved in their manufacture, must be improved [5, 6].

Solar cells based on plasmonics are an excellent solution for increasing industrial process operational efficiency and effectiveness [7]. An innovative method for achieving light trapping in thin-film solar cells is the use of metallic nanostructures that sustain surface plasmons [8]. Conduction electron excitations at the interface of a metal and a dielectric can be concentrated and folded over a thin layer of semiconductor material to increase absorption. Surface plasmons generated in metallic nanoparticles and surface plasmon polaritons (SPPs) propagated at the metal–semiconductor interface are both of intrigue [9].

Plasmonics has been combined with a variety of architectural configurations in recent years to improve the efficiency of thin-film solar cells [6]. Finite element analysis was used by researchers to investigate how different gold (Au) grating configurations affect the light-gathering capabilities of solar cells. The solar cell's architecture consists of an amorphous silicon substrate with a gold layer on top (a-Si). The grating device's periodicity was chosen so that it would be effective in activating surface plasmon polaritons (SPPs) [10].

To achieve the goal of increasing light absorption rate, a further plasmonic structure consisting of silver nanoparticles coupled with a silicon thin-film solar cell will be used. The goal of this structure is to enable sunlight into the cell from any angle while causing as little disruption as possible. Silicon is the light-absorbing layer, and when sunlight passes through it, the chemical bonds disintegrate and a large number of electrons are released due to the high absorption rate of this layer. These silver nanoparticles have a rounded shape. By concentrating plasmon resonances on the surface, their inclusion in this layer is intended to increase solar energy absorption [11].

Another method for producing the plasmonic effect is to incorporate plasmonic grating onto the surface of the solar cell. This method can be used to control the amount of light absorbed as well as detect light with a specific polarization. Plasmonic gratings increase absorption, are extremely efficient at reducing losses, and enable optoelectronic devices to transmit light power [12].

This research project provides and investigates the use of a plasmonic grating structure as the back metal contact or the rear electrode of thin film solar cells as an efficient method for increasing the efficiency of thin film solar cells. The grating surface causes light to be diffracted, resulting in a longer path for the light to take when reflected. The absorber layer is also linked to the amount of energy that surface plasmons have after being activated inside the grooves. Both efficient light trapping and surface plasmon resonance can improve absorption in a solar cell's absorber layer, resulting in a higher level of efficiency [13].

The various techniques for improving PV efficiency, including the most up-to-date structures and physics insight, are configured in this study. To achieve high-efficiency solar energy systems and solar energy management circuits, different design levels of circuits require the development of accurate and compact models for studying the behavior of photovoltaic cells under different conditions. The introduced models are divided into two categories: the first is based on the introduction of simple compact models to configure the main PV parameters and can be linked with any of the SPICE simulation tools that require short computational times even with less accuracy [14]. The second is based on the introduction of complex models that require longer computational times and less accuracy [15]. Both types are used for different purposes depending on the design requirements, and the two types of those models suffer from a lack of information about semiconductor physics aside from a few research articles [16, 17].

### The main contributions of this review paper are:

- In this survey, the thin film solar cells are broken down into two categories: classic and innovative technology. A contrast is shown between the many kinds of thin-film solar cells that have been created to improve efficiency.
- We will explore the major aspects of the different models.
- The different techniques for improving PV efficiency, including the most updated structures and physics insight, are configured.
- Exploring the major aspects of the different models,
- This survey contains a review of the available commercial software programmers for simulating thin-film solar cells.
- The survey concludes with a discussion of the difficulties that must be overcome to put thin-film solar cells into practical use.
- Exploring the different equivalent circuit models of thin film solar cells.

This survey's framework shown in Fig. 1 is introduced as follows: presents the "Related Work", presents the related work. The "Classification of Solar Cells" describes the various types of solar cells and presents compact models. The "Challenges, New Trends, and Future Work in Silicon Thin-film Solar Cells", followed by a comparison. Finally, the "Conclusion" contains the paper's conclusion.

Related Work

Several different research groups worked together to do extensive experimental work to address the challenges posed by solar cell materials. Although some review studies, such

Fig. 1 Arrangement of sections encapsulated in this paper
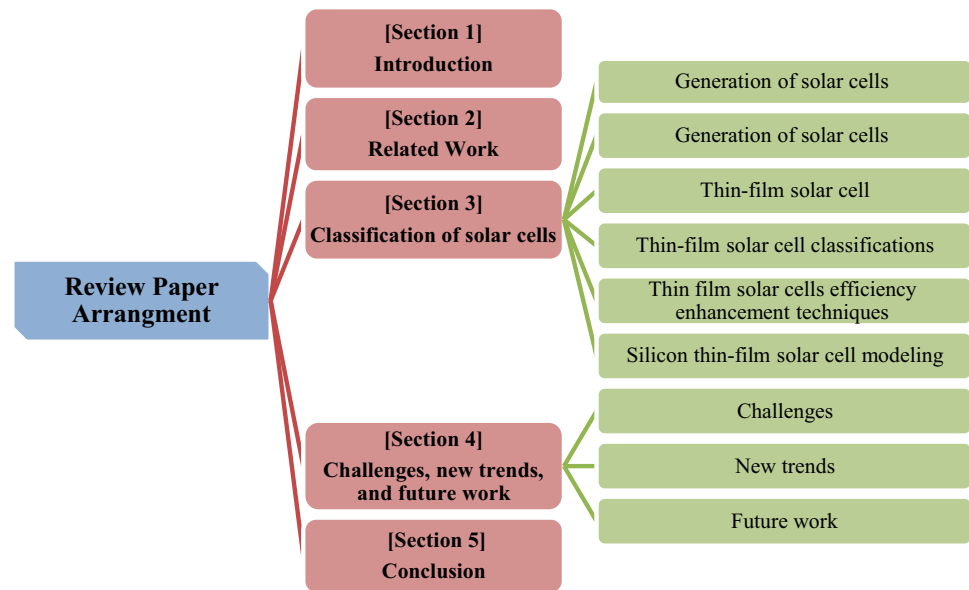
as Lee and Ebong [18] and Kowsar et al. [19], have reported on various major technologies, there is no comprehensive report that covers all aspects (such as efficiencies, developments, structure, requirements, and restrictions). As a result, a concise report which is structured and instructive, with distinct categories amongst classifications, will be greatly useful to the greatest possible word recognition. As a result, this article summarizes each cutting-edge technology that possesses all of the characteristics defined in the preceding section for the three basic types of thin-film solar cells.

Thin-film solar cells (TFSCs), also known as second-generation technologies, are created by applying one or more layers of PV components in a very thin film to a glass, plastic, or metal substrate. The film thickness can range from a few nanometers to tens of micrometers, making it significantly thinner than its competitor, a typical first-generation c-Si solar cell with thin films as thin as 200 nm [20].

The Si solar cell, which is initially deposited in a p-i-n structure, can also be produced in an n-i-p sequence [19]. The device's initials were p-i-n. This random crystal structure solar cell is typically manufactured on fluorine (F)-doped tin oxide (SnO_2:F)-fabricated glass substrate for single-junction applications or on a regular (honeycomb)-textured substrate (HTS) for micro morph (tandem) structure applications. Substrates are sequentially coated with silver (Ag) and gallium (Ga)-doped zinc oxide to reduce reflective loss and improve conductivity (ZnO: Ga). Then, diode or triode plasma-enhanced chemical vapor deposition is used to deposit hydrogenated-Si (-Si: H) using CO_2, diborane (B_2H_6), phosphine (PH_3), hydrogen (H_2), and silane (SiH_4) (PECVD). This method is used to create a transparent conducting oxide TCO film for front windows. This coating is made by RF magnetron sputtering from

indium tin oxide (In_2O_3: Sn) or hydrogenated indium oxide (In_2O_3:H) (IOH). A moth-eye-based antireflection coating (ARC) layer can improve cell performance after using Ag as the grid electrode [21]. The substrate type was used to stack (p) c-Si: H [21]. The tandem (triple-junction) device [HTS/Ag/GZO/c-Si: H/c-Si: H/c]. The triple-junction module cells were isolated using reactive ion etching and nano-crystalline silicon oxide (nc-SiO_x) layers. A hydrogenated micro-crystalline Si (c-Si: H) cell with a thickness of 1.8 mm at the bottom, 1.6 mm in the center, and 230 nm at the top was used in the apparatus [21].

The α-Si solar cells are afflicted with:

1. Improve the deposition method, which is required for large-scale production of the solar cell [22].
2. Improve the optoelectronic properties of the front transparent conducting oxides TCO component to address light scattering qualities [23].
3. A Staebler-Wronski effect solution must be revealed by determining a suitable strategy for avoiding light-induced deterioration of the device structure [24].

In the case of the -Si: H solar cell, the formation of an electron–hole pair in the intrinsic layer as a result of photon absorption results in the induction of an electric field across the intrinsic layer. This induces the movement of electrons to the n-layer and holes to the p-layer, respectively. To improve cell performance, it is common practice to use an interface layer that is both thin and graded. This helps to lower the number of p/i interface faults that lead to a low open-circuit voltage (Voc) and short-circuit current (Jsc), and it also helps to reduce the number of p/i interface deficiencies.

Fig. 2 Categories of solar cell technologies [25]
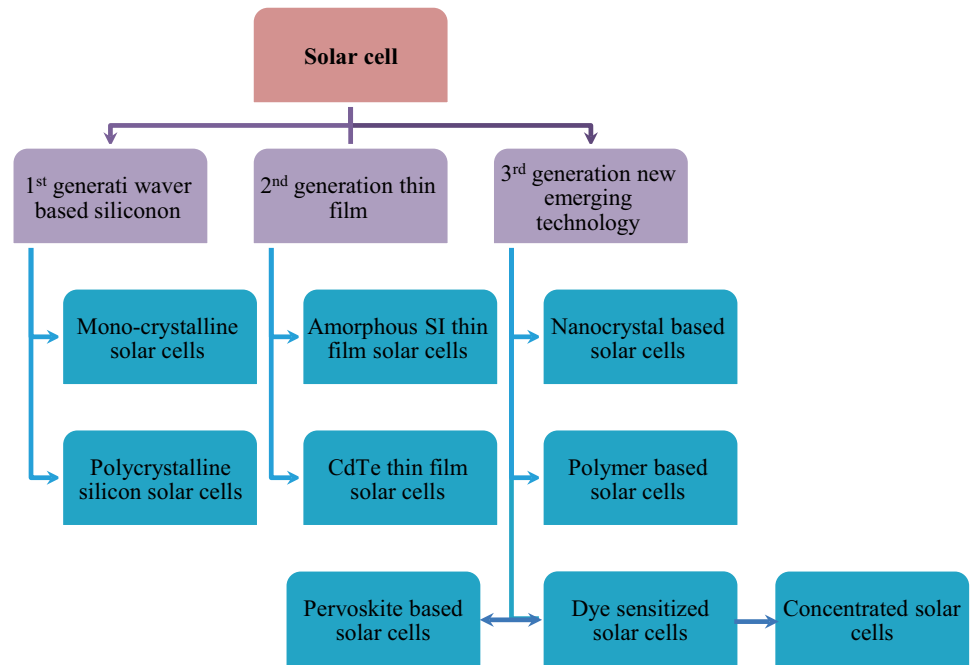
Classification of Solar Cells

Figure 2 depicts the three primary types of solar cells based on the technology used and the method of manufacture:

The first generation of solar cells is constructed from crystalline silicon wafers, which have a low power conversion effectiveness of 27.6% [26] and a relatively high manufacturing cost. Thin-film solar cells have even lower power conversion efficiencies (PCEs) of up to 22% because they use nano-thin active materials and have lower manufacturing costs [27].

Generation of Solar Cells

The data required to assess the behavior of various solar cell generations is shown in Table 1: By about 15–20%, first-generation solar cells outperform second-generation solar cells. The materials utilized by the second-generation solar cell, which has a performance range of 4–15%, include amorphous silicon, CdTe, and CIGS.

These techniques are significantly less expensive than first-generation technologies because they do not use silicon wafers. First-generation solar cells have higher proven efficiencies than thin-film solar cells; however, first-generation solar cells are more expensive because pure silicon is used throughout the manufacturing process.

Thin-film solar cells, on the other hand, are more efficient, require fewer resources, and produce results in a shorter amount of time. Also, they are less expensive. First-generation solar cells, in contrast to second-generation solar cells, are abundant and do not emit harmful by-products during their operation. In comparison to earlier generations of solar cells, those of the second generation have both a lower cost per watt and a higher efficiency. The third-generation solar cell is constructed of organic materials and polymers to make it more durable. The solar cell of the third generation is more efficient and less expensive than those of earlier generations. Even though it has not yet been verified, the procedure for generating cells of the third generation is straightforward and offers innovative new technology. In recent years, a brand-new solar cell technology has evolved, most notably the perovskite solar cell, which achieves record efficiencies of more than 25% and possesses immense potential.

Table 1 Three different thin film materials' physical properties

Parameter	a-Si	CdTe	CIGS
Absorption coefficient	1.7442×10^6 cm^{-1}	1.1148×10^6 cm^{-1}	$> 1 \times 10^5$ cm^{-1}
Bandgap	Direct 1.75 eV	Direct 1.44 eV	Direct 1.0 eV−1.6 eV
Sufficient thickness	1 μm	3–5 μm	1–2 μm
Temperature coefficient	−0.3%/°C	−0.25%/°C	−0.26%/°C
Toxicity	None	Cadmium	None

Thin-film Solar Cell

The use of less material is linked to an increase in energy conversion efficiency, both of which contribute to lower overall costs. Wafer technology has the highest efficiency, while thin film technology has the lowest material consumption. Both technologies are capable of achieving both of these goals. Both of these goals must be met at the same time to produce power at a low cost and enable significant market penetration of solar electricity. Both of these objectives are interdependent. The three most widely commercialized thin film solar cell technologies are CIGS, a-Si, and CdTe.

The straight bandgap (Table 1) is a property shared by all three of these materials, and it is this property that allows for the use of extremely thin materials [28]. Wafer technologies, on the other hand, are not hampered by low light intensity, despite having a very low-temperature coefficient. This is due to wafers' extremely low-temperature coefficient. This is because wafers are made of extremely thin layers of material. Furthermore, all three of these technologies can be used to create photovoltaic systems for buildings (BIPV). Amorphous silicon solar cells are commonly utilized in a wide range of consumer electronic products [29], such as calculators, watches, and other similar items.

When compared to their crystalline counterparts (Table 2), the absorption coefficients of thin film materials are markedly smaller than those of thicker counterparts. When compared to CdTe and CIGS, the toxicity of a-Si is considerably lower, and it also demands less silicon. CdTe contains cadmium, which is toxic to both the manufacturer and the customer [30], limiting the compound's potential commercial applications. Beta-Si has had the longest commercial lifespan of any material in human history since its introduction in the late 1980s [31] as a reliable power source for various semiconductor-based systems. This is because beta-Si has been used in electronic devices. However, CdTe and CIGS are considered new technologies that show greater promise than a-Si in terms of energy conversion efficiency. This is because CIGS and CdTe are both newer technologies. Both of these technological breakthroughs can be found here. Despite this advantage, the efficiency and dependability of CIGS and CdTe technologies are not yet on par with their crystalline silicon counterparts.

Thin-film Solar Cell Classifications

A-Si Solar Cell Structures and Materials

It has a direct bandgap, allowing for significant solar radiation absorption in only a few micrometers of material [47]. Electrical behavior and minority carrier diffusion lengths in amorphous materials are caused by dangling bonds and short orders. Hydrogen passivation, also known as a-Si: H can reduce dangling bond concentrations significantly. The hydrogenation effect, on the other hand, causes the Staebler-Wronski light degradation effect. Hydrogenated a-Si: H optical absorption spectrum is transparent up to 1.7 eV and strongly absorbent at 2 eV. Another advantage of silicon is its short payback period and low energy production costs. H. Wronski and Carlson invented the first solar cell with 2.4 percent energy conversion efficiency in 1976 [48]. An indium-tin-oxide (ITO)-coated glass substrate was deposited at temperatures ranging from 250 to 4000 degrees Celsius. Significant diffusion lengths are possible for both majority and minority carriers due to the comparatively thick intrinsic layer between the thinner n-type layers and p-type. Boron levels (0.1–1 ppm) are common in the i-layer, which is typically 250 to 500 nm thick. The intrinsic layer of the absorber generates an electric field, which separates and collects the electric charge [49]. To compound matters, the doped areas are extremely thin. Phosphorus-doped Si: H is also referred to as phosphorus-doped microcrystalline silicon. The n-layer, which is approximately 20–30 nm thick, is composed of Si: H. The p-layer is a hydrogenated boron-doped amorphous silicon-carbon alloy. The rear contact is sputtered or vaporized with aluminum. Carlson and Wronski [48] demonstrated this in 1976 by creating the first p-i-n-Si solar cell. This was the initial step in the development of laboratory Si solar cells. The theoretical maximum efficiency of a Si solar cell was estimated to be 14–15% based on this configuration.

A 4% increase in efficiency was announced in [49]. P-i-n diodes had 4.8% efficiency when Wilson [31] used Schottky diodes. Figure 3. Instead of p-n semiconductor junctions, the Si solar cell uses a metal-to-N junction [31]. In this type of solar cell, a Schottky barrier is used between the intrinsic region of a-Si and the Schottky barrier height function metal, resulting in highly doped p-type a-Si. This improves the Jsc and Voc Schottky barriers of the Si solar cell [50]. In 1980, Carlson considered a 6% p-i-n structure efficiency and a 6% Schottky structure efficiency.

Tawada et al. [51] discovered hydrogenated a-Si: H in 1982, paving the way for the expansion of -Si with an efficiency of 8.04 percent. Yablonovitch and Cody's [52] discovered light-trapping features [52]. Yamazaki et al. [53] discovered that hydrogenated a-Si: H resulted in a 9.3 percent efficiency increase in 1986. Multiple wavelengths of response were possible due to numerous bandgaps in multi-junction cells and modules developed in the early 1990s (Figs. 4 and 5). When a photon's energy is less than that of a semiconductor's bandgap, it is not absorbed by the semiconductor. Bandgaps in multi-junction technologies can be easily changed by alloying changes, but a larger bandgap at the top of the stack is required. Energy can be captured that would otherwise be lost in

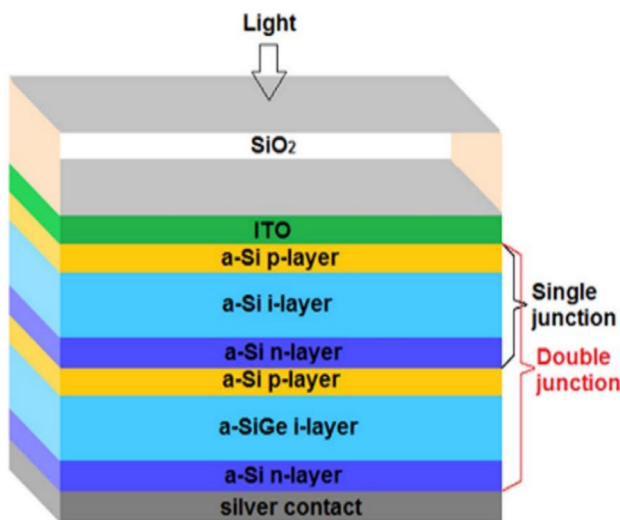**Table 2** Comparison of various types of solar cell technology

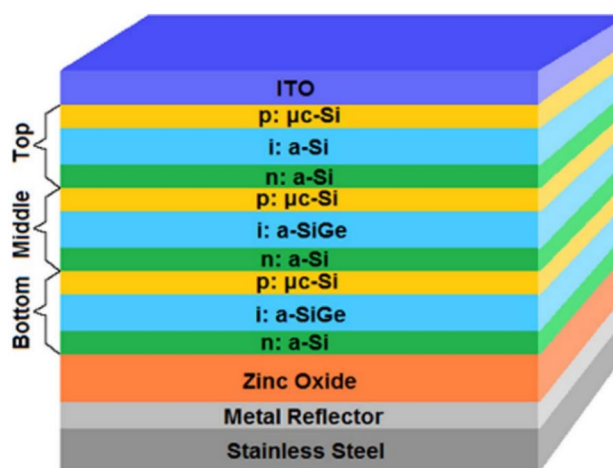| Type of cell	Size	Cost	High-temperature performance	Temperature coefficients	Efficiency	Other details	References
First-generation							
Monocrystalline solar cell	Using less space to get the same level of performance	Cost twice as much as thin-film solar cells and are more expensive than crystalline silicon	Has poor performance in hot conditions (drops 10–15%)	0.003–0.004/K	17–18%	Traditional, yet ubiquitous, solar cell technology	[32, 33]
Polycrystalline solar cell	Reduces space while maintaining output efficiency	Costing twice as much as thin-film solar cells yet produces the same amount of energy as cheap crystalline silicon	Has poor performance in hot conditions (drops 20%)	0.0042–0.0045/K	12–14%	The Cost-Effectiveness Ratio Encourages a Practical Decision	[34, 35]
Second-generation							
a-Si (amorphous silicon)	Product designs range from flexible and lightweight to sturdy and long-lasting	It's 50% less expensive than crystalline silicon	Holds up well in both low (0% drop) and high temperatures	0.0011–0.0026/K	4–8%	Installation time is longer than with other competing technologies	[36–38]
CdTe	Product designs range from flexible and lightweight to sturdy and long-lasting	The most cost-efficient option, and one that is 50% cheaper than crystalline silicon	Works as well in low (0% drops) and high temperatures	0.0022–0.0025/K	9–11%	Dangerous because it was made with Cd	[27, 39]
CIGS Solar cells	Product designs range from flexible and lightweight to sturdy and long-lasting	It's 50% less expensive than crystalline silicon	Workable in both low and high temperatures	0.0035–0.0036/K	10–15%	Efficiencies of 20% have been reached by some CIGS	[40, 41]
Third generation							
Nano Crystal solar cells	Product designs range from flexible and lightweight to sturdy and long-lasting	It's 50% less expensive than crystalline silicon	Demonstrates remarkable resistance to temperature changes	- N.A	7–8%	Fast assembly time, but lots of room is needed for installation	[5, 42]
Polymer solar cell	Product designs range from flexible and lightweight to sturdy and long-lasting	It's 50% less expensive than crystalline silicon	Having trouble functioning in hot environments	- N.A	3–10%	Fast assembly time, but lots of room is needed for installation	[25, 43]
Dye-sensitized solar cell	Product designs range from flexible and lightweight to sturdy and long-lasting	It's 50% less expensive than crystalline silicon	Having trouble functioning in hot environments	- N.A	9–10%	Installs quickly and takes up little room	[44, 45]
Concentrated solar cells	Providing expert product design services in a variety of fields	To save half the cost of a regular Si cell	demonstrates remarkable resistance to temperature changes	- N.A	39–40%	Requires a huge area and lots of time to set up	[40, 46]
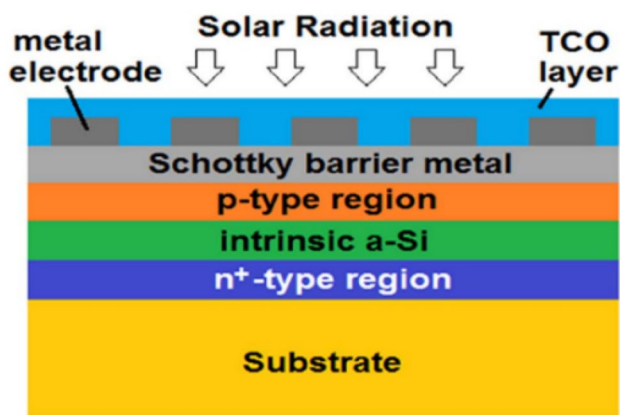
Fig. 3 The a-Si Schottky barrier solar cell design. In this case, we have an a-Si Schottky barrier solar cell with the area adjacent to the Schottky barrier high work function metal strongly doped to p-type

Fig. 5 Design of a triple junction Si: H/-SiGe/-SiGe Solar cell

single-junction solar cells. It has also been demonstrated that optically connecting two mechanically distinct Si cells in series can improve performance [54].

Furthermore, multi-junction technologies are less susceptible to light-induced deterioration. Guha et al. demonstrated multiple-junction solar cells using the multi-junction concept. Yang et al. accomplished stable conversion efficiencies of 11.8 percent and 13 percent in 1996 and 1997, respectively, using a "spectrum splitting, triple-junction arrangement." A dual junction and low-bandgap Si: H/Si: Ge alloyed cell enabled this advancement in laboratory a-Si solar cell technology (Fig. 6). To improve electric generation and current transfer within the cell, a more effective TCO, also recognized as the best conducting oxide, was developed, in addition to a p-n tunnel junction between the component cells [55].

According to the study in [56], utilizing hydrogenated microcrystalline silicon (c-Si: H) and hydrogenated silicon dioxide (H2O2) in three various layers of the solar cell resulted in a 13.4 percent accuracy to use a stable a-Si: H solar cell. Sai et al. [56] explored equivalent triple junction technologies using a Si: H/c-Si: H cell and accomplished a stabilized efficiency of 13.6 percent. Honeycomb-textured substances (also known as "honeycomb-textured substrates") have been employed to enhance light trapping in multi-junction technologies, leading to a substantial rise in PCE [56]. Given these advancements, it is evident that a-Si: H technologies have played an essential part in the development and invention of triple junction technology, as well as how these technologies are going to be utilized in the future. The cell's power conversion efficiency has improved as a result of the use of various semiconducting materials.

Fig. 4 A double junction layout Solar cell a-Si: H/a-SiGe: H
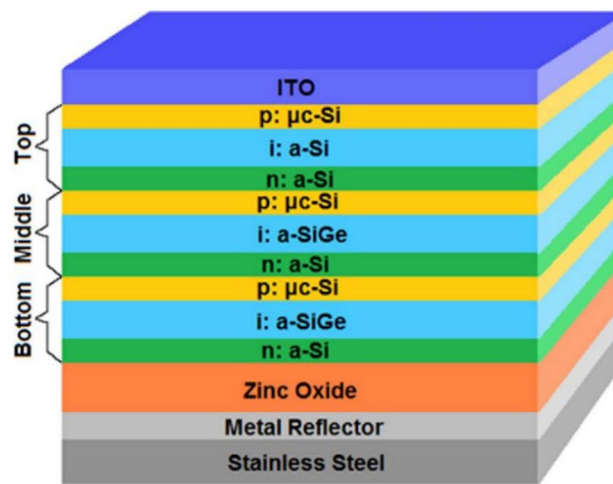
Fig. 6 (-Si: H/-SiGe/-SiGe) A triple junction solar cell layout

CIGS Solar Cell Structures and Materials

Figure 7 depicts the CIGS structure on soda-lime glass. On the glass surface, molybdenum interacts with p-type Cu (InGa) Se2. The primary junction consists of an n-type CdS buffer and a p-type Cu (InGa) Se2 [57]. The n-type ZnO: Al layer acts as the front contact on top of the CdS. This solar cell's semiconductor is between 1.24 and 4.04 m in size, while crystalline silicon is between 170 and 200 m. When an in-finger contact was used as the top electrode, 75% of the incident radiation was allowed through, increasing efficiency to 5.7 percent. The improved performance was due to improved junction characteristics and increased carrier absorption through the CdS window. Because the lattice parameters of CuInSe2 and InP matched those of CdS, interfacial states were reduced. Ideality factor and high series resistance, as well as grain-boundary recombination that reduced Jsc, all contributed to the observed sub-10% efficiency. Chen and Mickelsen [58] developed a CdS/CuInSe2 heterojunction solar cell with 5.7 percent efficiency in 1980. The Jsc of 31 mA/cm2 was achieved without the use of an antireflection coating (ARC) layer (ARC) in this cell. The low open circuit voltage and high Jsc were caused by the band bending and Fermi position in high-resistivity CuInSe2 (Voc). Chen and Mickelsen [59] improved performance by combining p-and n-type CdS with CuInSe2. Because of the presence of two selenide layers and 10% CdSe in the CdS layer, this structure is unique.

By increasing selenide resistivity and decreasing photon losses, they were able to demonstrate a cell with 10% efficiency. Chen and Mickelsen [60] were the first to illustrate thin-film CuInSe2/CdS solar cells in 1981. Variation in selenide layer evaporation increases effectiveness. While the rates of In and Se deposition remained constant, the rate of Cu deposition was adjusted to achieve the desired composition and resistivity. Recombination pervades interface
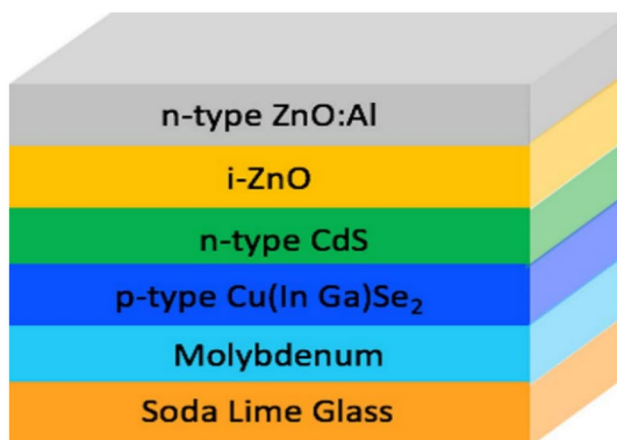
Fig. 7 The CIGS solar cell structure

transport, and low Voc was attributed to high Se resistivity. Cells were annealed in H2/Ar and then in pure oxygen to better understand the limitations of cell function. Jsc increased in all three situations as a consequence of the heat effect, whereas Voc and FF enhanced only in an oxygen-rich environment. After deposition, baking the cells in air or oxygen at 200 degrees Celsius improves their performance.

Mickelsen and Chen [61] increased Voc and Jsc efficiency by 10.6% by using ZnxCd1xS. A high Jsc was obtained due to good crystallinity at the selenide-sulfur interface and the absence of any undesirable planar grain boundaries. Because zinc increased electron affinity between the selenide and sulphide layers, its presence in the sulphide layer increased Voc. Potter et al. [62] achieved 11.2% efficiency by combining ZnO with p-type CuInSe2 and undoped(Cu, Zn)S or CdS. Jsc was enhanced by 25% with a ZnO anti-reflective coating, while a thin film of CdS absorbed light at 520 nm. In 1988, Mitchell and Liu [63] increased Potter's effectiveness by one percentage point, to 12.2 percent. By adding texture to ZnO, the amount of optical reflection was diminished to 6%. Annealing, which reduced the resistivity of the CIS film, and a direct bandgap of 1.0 eV, which increased photocurrent, both increased efficiency by 1%. Devany et al. [64] used the quaternary compound CuInGaSe2 to replace the ternary CuInSe2 in-dependent bandgap. The quaternary CuInGaSe2 layer was used to increase Voc and decrease infrared absorption losses in ZnO, resulting in a 12.5% increase in efficiency.

For the majority carrier collection, Chen et al. [65] revealed an efficiency of 13.7% in 1993 using quaternary (CIGS) as the p-type absorption, CdZnS mixed alloys as the n-type layer, and ZnO transparent conducting oxide as the n-type over-layer. Boosting the substrate temperature (above 500 °C) enhanced CIGS efficiency. By diminishing wasteful reflection, lowering wasteful ZnO absorption, and rising selenide Ga content, an efficiency of 13.7% was accomplished. In 1994, Gabor et al. [65] revealed a 15.9% CuInxGa (1x) Se2 solar cell efficiency. Tuttle and colleagues [66] achieved 17.7 percent efficiency by using molecular back contact as a channel for impurity migration from glass to the absorber and a sputtered ZnO emitter coated with MgF2 as a channel for impurity relocation from glass to the adsorbent. The increased Voc is caused by reduced recombination in the CdS conduction band and a thinner CdS layer, which shifts the absorber band edge to higher energies. In 1999, Contreras et al. [67] reported an an18.8% efficiency after optimizing the ZnO window layer, improving the CIGS absorber-CdS buffer layer interface, increasing minority carrier mobility length, and lowering space-charge recombination.

ZnO/CdS/CuInGaSe2 thin-film cells accomplished 19.2% efficiency when Ramanathan et al. [68] used bandgap grading of Ga and In to boost Voc. In 2005, Contreras et al. [69]

reported a 19.5% performance in CIGS solar cells. Enhancing the absorber bandgap to 1.14 eV, accomplishing a low diode saturation current density (J02) of 3108 mA/cm2, and achieving an ideality factor (n-factor) of 1.30 to 1.35 resulted in a better cell. Repins et al. [70] achieved a 19.9% efficiency by narrowing the bandgap in the space charge area.

Thus, the Voc concentration was identical to that identified by Contreras [69], but the FF was 81.2%, with an ideality factor of 1.14 and a specific conductance (Jsc) of 2.1109 mA/cm2. The authors observe in 2010 that CIGS cells with metal connections of 4 nm were 20.3% efficient [71].

In 2013, EMPA [72] created a thin-film CIGS solar cell with 20.4% efficiency on a flexible polymer substrate. Roll-to-roll continuous cell production is enabled by a thin CIGS layer on a polymer substrate. In their study, Powalla et al. [73] demonstrated that a cell made by static co-evaporation could achieve a 20.4% efficiency. Between the CIGS layer (which absorbs light) and the ZnO front electrode was a Zn (O, S) buffer layer (which is transparent). They use a high-vacuum cluster deposition setup for static co-evaporation of CIGS absorber elements as well as sputter deposition of ZnO and i-ZnO: Al for the windows. Powella et al. [74] discovered that doping the Cu (In, Ga) Se2 layer with potassium increased efficiency by 20.8%. The novel doping method allowed for a higher gallium concentration in the CIGS absorber without sacrificing performance. The new deposition technique reduced the effects of Voc saturation and changed the composition of the CIGS absorber to increase the concentration of gallium. The development of higher-bandgap CIGS cells was halted when the Voc was saturated with increasing Ga content. Herrmann et al. [75] reported 21 percent of CIGS cells were in 2014. The rate of CIGS deposition was increased, resulting in a significant increase in efficiency. Jackson et al. [76] discovered a productivity rate of 21.7% in 2014. Optimization of alkali post-deposition treatment improves cell performance [77]. Solar Frontier increased efficiency to 22.3% [78] by optimizing the CIS absorber layer and connection fabrication process.

CdTe Solar Cell Structures and Materials

CdTe thin-film solar cells have high efficiency. The compound is stable and has a direct bandgap, similar to CIGS. Thin CdTe films have the potential to produce high-efficiency cells if bulk and surface recombination are kept to a minimum. Bonnet and Rabnehorst built the first large experimental CdTe cell in 1972, which had a 6% efficiency. The cell shown in Fig. 8 was created using CdTe vapor-phase deposition and CdS high vacuum evaporation [79]. Jsc can be increased with enhanced photo-carrier transfer thanks to a graded gap junction. The Molybdenum Mo-CdTe back contact proved difficult for Bonnet and Rabnehorst due to the enormous series resistances and low FF caused by using pure Molybdenum (pure Mo).

To make a non-rectifying contact on a wide-bandgap p-type semiconductor, a high-function metal must be used, as well as local doping of the semiconductor near the contact metal. Charge carriers can tunnel through the resulting thin depletion layer. The sudden surge in the popularity of the technology resulted in a plethora of CDT fabrication procedures.

In 1976, Nakayama et al. [80] investigated the feasibility of screen-printing on CdTe solar cells. Ceramic films of In2O3 and CdS were implemented on the glass's surface. Because CdS served as an ohmic transparent electrode, series resistance, and surface recombination were reduced in the CdTe layer. It boosted the effectiveness of a CdTe solar cell to 8.1% [75]. Bube and colleagues [81] investigated 8.4% efficient CdS/CdTe solar cells. The n-CdS/n-CdTe/p-CdTe junctions in this structure were formed during junction formation by the diffusion of n-CdS donors into p-CdTe, with the CdS film acting as a contact to the CdTe homojunction. The interface recombination velocity can be diminished by raising the CdTe acceptor doping concentration to 1017 cm3. Solar cells made of CdS/CdTe are less expensive than silicon solar cells. Eastman Kodak Company patents [82] show that by stacking polycrystalline CdS and polycrystalline CdTe, 8.9% conversion efficiency was achieved. When exposed to oxygen-containing air, the incorporation of oxygen atoms into the sublimating semiconductive layer improved the device's performance. Following that, incorporating oxygen into semiconductor layers improved performance by 10.5%. The p-type CdTe layer is strengthened by oxygen, ensuring shallow-junction behavior.

Eastman Kodaks's Tyan and colleagues [83] were able to achieve a 10% efficiency by incorporating tellurium between the p-type CdTe and the metal contact. CdTe grain boundaries are depleted in cadmium near the tellurium layer. According to both theory and practice, the junction preparation strategy governs the integrity of the resulting cellular junctions. In CdS, heterojunctions are formed through vacuum evaporation, whereas buried homojunction is formed through chemical vapor deposition. In 1983, Werthen et al.
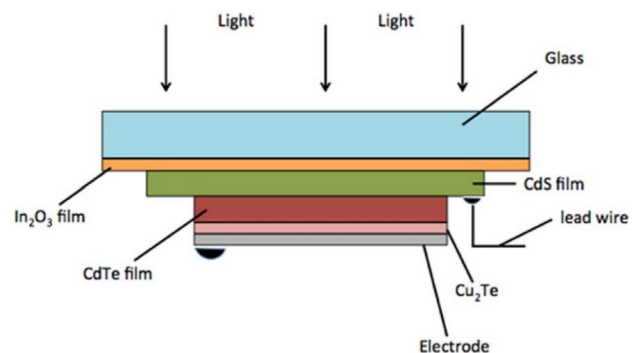
Fig. 8 A ceramic thin film CdTe solar cell schematic cross-section [79]

[84] demonstrated that low-doped CdTe increased Voc. In contrast, low-doped CdTe increased recombination in the depletion area while decreasing recombination at the interface. Werthen and colleagues discovered that using low-doped CdTe is a viable option for all CdTe solar cells and that heating the semiconductor layers may improve performance. In 1984, Kuribayashi and colleagues [85] improved device efficiency to 12.8% by using carbon electrodes and oxygen during CdS and CdTe deposition to reinforce the p-type CdTe film and ensure shallow junction behavior. The contact resistance between the CdTe and carbon electrodes was reduced and the CdTe layer was strengthened by including an appropriate amount of Cu (50–100 ppm) in the carbon paste during carbon diffusion into the CdTe layer during heat treatment. The Energy Department revolutionized CdTe solar cells in 1987.

Previously, efforts were focused on improving electrode placement, screen printing, and sublimation in confined spaces. Closed-space sublimation at low vacuum and moderate temperatures allow for simple deposition setup and transport. Although p-CdTe heterojunctions had previously been created, their short minority carrier lifetimes and low resistivity connections rendered them ineffective. Meyers and colleagues at Ametek [86] proposed a novel n-i-p design with many advantages over top-of-the-line CdTe heterojunction devices. The high-resistance CdTe used in these cells outperformed the low-resistance sheets used by other manufacturers. Instead of using low-resistance connections, rectification was used, and the i-layer field aided in charge carrier collection. Two examples are n-type CdS and p-type ZnTe. Unrestricted hole flow is possible due to a small break in the valence band edge at the CdTe/ZnTe interface. Productivity increased quickly, increasing the effectiveness by 10.4% [87]. An ohmic contact is difficult due to the large work function of CdTe. As a result, as a buffer layer, p-ZnTe was used. The cost of CdTe solar cells became more important in their commercialization as their efficiency increased. The development of low-cost, high-throughput manufacturing methods for high-efficiency CdTe solar cells is a popular research topic, and many labs are working to develop them. Bottenberg and colleagues at Arco Solar [87] created a three-layer system that included an intermediate dielectric layer, a front conductive layer, and a CdS-free semiconductor layer (a transparent conductor with a wide bandgap to eliminate the need for a CdS layer). The productivity increase was 10.5%. Chamberlin and his colleagues at Photon Energy increased efficiency to 12.3 percent [88]. The density of holes in properly doped CdTe is 2.8×10^{16} cm3. The device's efficiency was increased by lowering the contact resistance of the CdTe surface via chemical rinsing and etching. When Tottszer et al. [89] widened the band gap between the two materials, the efficiency of CdS/CdTe solar cells increased to 13.1%. By lowering the electric field at the

junction, the ability of the mid-gap recombination sites to trap light-generated electrons was improved.

Chu et al. increased efficiency to 13.4 percent [90] by developing low-resistivity p-CdTe films and establishing stable low-resistance connections. CdS films were created using a solution of cadmium salt, ammonium salt, and thiourea. We got CdS surfaces that stuck like glue and were also glossy and reflective using Chu's method. Chu developed a device with a 14.6% efficiency [91]. The material's remarkable efficiency was attributed to an interface reaction between CdS and CdTe during high-temperature CdTe deposition. The electrical connection was moved to CdTe due to the formation of CdSxTe1x at the contact, which improved the material's photovoltaic capabilities. To achieve high solar conversion efficiency, the chemistry at the CdS/CdTe interface must be strictly regulated. After refining Chu's methods, USF researchers Britt and others [92] reported 15.8% efficiency. In Fig. 9 because of the high temperature used in CdTe deposition via close-spaced sublimation, CdS and CdTe may interdiffusion (CSS). To separate the electrical junction from the metal-liquid junction, CdxS1xTe was used. As an additional electrical contact, a graphite paste containing mercury was used. Britt et al. [92] revealed that pre-deposition annealing of CdS layers in H2 raised grain size, reduced interface states, and enhanced bandgap energy by 0.12 eV. The thickness of CdS films can be decreased or removed due to the Cd-rich surface left by annealing, which aids in the prevention of shunting channels from Figs. 10 and 11.

Thin Film Solar Cells Efficiency Enhancement Techniques

One of the primary goals of solar cell research and development should be increased power conversion efficiency (PCE). The Shockley and Queisser model predicts a single-junction solar cell efficiency of 33% [93]. In a single-bandgap solar cell, only incident photons with energies greater than or
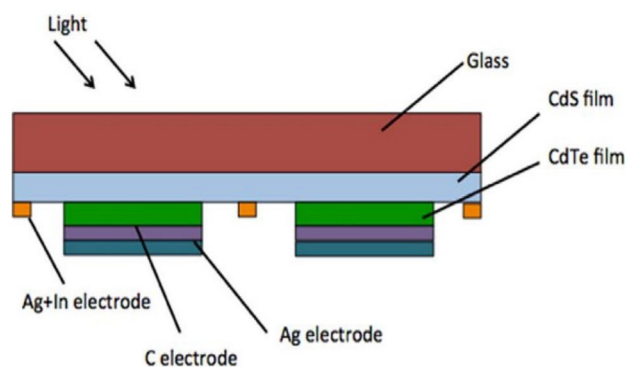

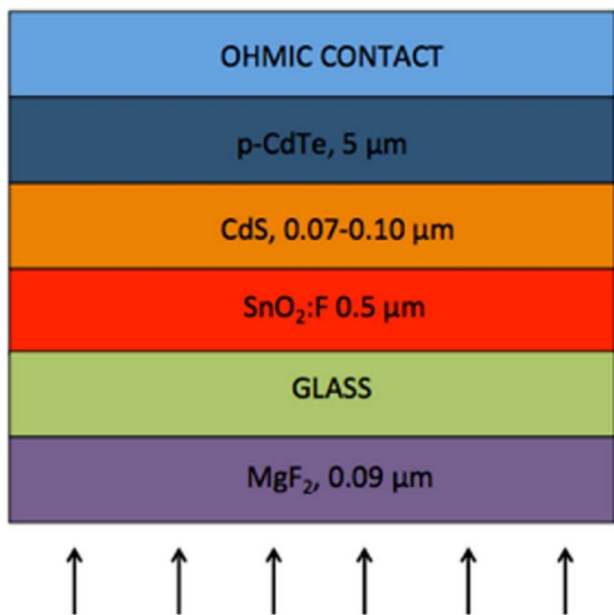**Fig. 9** CdS/CdTe solar cell cross-section [92]

Fig. 10 Thin-film CdTe solar cell configuration [92]

equal to the bandgap of the active material generate electrical energy [94]. Lower-energy photons cannot activate the solar cell and thus are wasted. As a result, single-band gap solar cells are less efficient than those with multiple gaps. Luque and Marti's [95] concept of intermediate band solar cells (IBSCs) can be used to improve power conversion efficiencies. This enhancement can theoretically reach a value of 63.2%, which is higher than the highest efficiency value attained by other solar cell types [96].

Many theoretical and experimental studies have shown that incorporating quantum dots (QDs) into the active layers of solar cells can improve their efficiency [97]. The efficiency of quantum dot intermediate band solar cells (QD-IBSCs) is the greatest of any IBSC type described in the scientific literature to date [98]. Carriers can be stored in QD-IBSCs, according to conventional wisdom, by forming an intermediate band (IB) in the energy gap between the QD's conduction band offset (CBO) and the valence band (VB) [99]. A tiny amount of doping in the region where
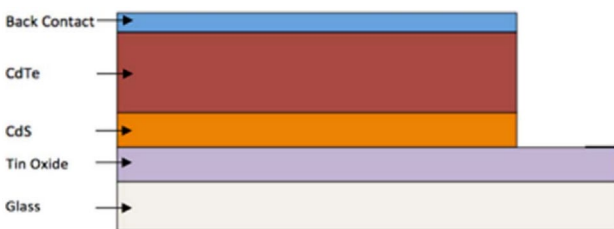

Fig. 11 CdTe/CdS thin film solar cell structure [92]

the IB is formed is required for the greatest potential transmission of carriers across the IB. Controlling the doping in the layers surrounding the IB allows you to control its thickness [100].

The literature [100] has established that QD-IBSCs increase the photo-generated current in PV cells via a multistep improved light absorption process. Although short circuit current density (Jsc) rises, open circuit voltage (Voc) falls as expected [101].

Surface Grating Techniques

According to the research that has been conducted, the usage of a surface grating is one of the light-trapping tactics that may be implemented in a solar cell to improve both the photo-generated short-circuiting current as well as the open circuit voltage [102]. Surface gratings with IBSCs may thus be considered an appropriate option for compensating for the decrease in Voc caused by the addition of QDs with a low effective bandgap to a solar cell's active material structure.

The purpose of the solar cell's surface grating, according to Fig. 12 [103], is to enhance the optical path length of light waves within the active material by generating more internal reflections. When light strikes a solar cell's grating surface, some of it is absorbed by the active material in the cell, while the rest is reflected in the surrounding environment. When light is absorbed by the solar cell, it travels to the cell's bottom and is reflected up to the surface by the reflector on the cell's backside. Multiple reflections occur at the surface, increasing the optical length of the light wave path and, as a result, absorption [104]. The use of a triangle- or pyramid-shaped surface grating has been shown in the literature [105] to maximize the efficiency of a solar cell [38].

Surface Plasmons

The free-flowing electrons in metals are primarily responsible for the synergy between these materials and electromagnetic waves. In this model, free electrons fluctuate in a way that is 180 degrees out of phase with the electric field that generates them, as opposed to the basic Drude model's 90 degrees in phase. The high reflectivity of metals is because their dielectric constant is negative at optical frequencies. Furthermore, at optical frequencies, surface and volume charge density oscillations, known as plasmons or plasmon polaritons with distinct resonance frequencies, may be observed in the metal's free electron gas. Plasmons are commonly observed when light interacts with metal nanostructures, but they can also be found in other situations [106].

Because material properties vary with frequency, it is not feasible to merely recreate the same performance in different spectral ranges using Maxwell's equations' scale invariance. This also implies that the outcomes of optical frequency
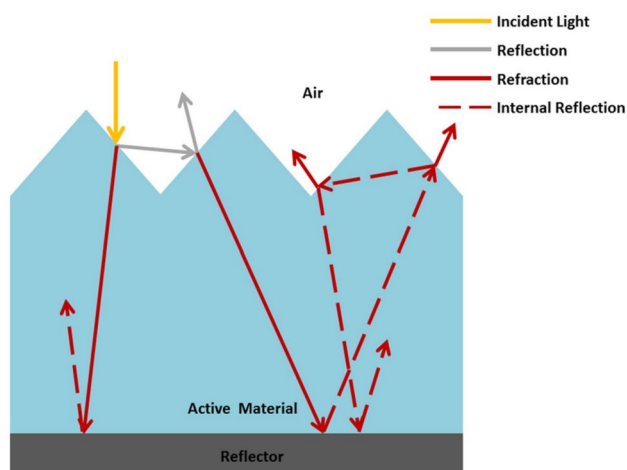
Fig. 12 The effect of surface grating on solar cell absorption [103]

testing with metal nanostructures cannot be extrapolated from model experiments with, say, microwaves and correspondingly larger metal structures.

Surface charge density oscillations that are brought on by surface plasmons at the metal–dielectric interface have the potential to bring about greatly enhanced optical near fields that are spatially confined near a metal surface. The total displacement of electrons relative to a positively charged lattice produces a restoring force when an electron gas is confined in three dimensions, such as in a small sub-wavelength-scale particle. This leads to the formation of particle-plasmon resonances, which are dependent on the particle's geometry. A substantial amount of local charge can be accumulated on particles with the appropriate shape, which is often pointed. This charge can then be amplified by optical fields that are far stronger [107].

Plasmonics and nano-plasmonics are new terms used to describe the study of optical phenomena related to metal electromagnetic responses. In recent years, there has been a surge in interest in the sub-wavelength scale limitations of optical radiation, a rapidly developing field of nano-science.

Merging of Plasmonics and Nano-photonics

It has become clear over the last decade that plasmonics could play a significant role in future device technologies, acting as a complement to existing photonics and electrical technologies. In other words, plasmonics contributes precisely what photonics and electronics do not require, namely the speed of photonics and the size of electronics [107] as shown in Fig. 13. The dashed lines represent the physical constraints of various plasmonic-derived technologies.

In Fig. 14, the Plasmonic devices can interact logically with photonic and electronic components that work at speeds comparable to their own, which would increase

the synergy between these technologies and the applications they discover.

Plasmonics may be exploited as a result of this fact to bridge the gap that exists between high-speed dielectric photonics and nano-electronics that are comparable in size and scale. Circuits and systems that are constructed from plasmonic and electronic devices have a high level of certainty for usage in next-generation systems because of the inherent integration compatibility that plasmonics has with electronics and the speed that photonics provides. This is because they will combine the most beneficial aspects of both photonics and electronics to facilitate multiplication and communication at fast speeds, broad bandwidths, and with a low level of power dissipation. Plasmonics offers a high level of certainty for the next step in technology development as a result of its inherent integration compatibility, which is another point that must be emphasized [109].

In the last decade, a wide range of plasmonics applications have emerged, and they are now widely regarded as promising areas of development. However, it is beyond the scope of this thesis to discuss all of the promising areas of development. Several excellent reviews, including those by Atwater [109], Ozbay [110], and Maier [111] provide insights into current research as well as plausible applications such as plasmonic chips [112], nanolithography [113], waveguides and optical microscopy [114], and sensor and biosensor devices [115].

Plasmonics for Enhanced Photodetection

The basic goal of light trapping techniques is to increase absorption while limiting incoming light reflections to maximize the efficiency of a solar cell. Several plasmonic-enhanced photodetectors have been developed in recent years, ranging from a C-shaped germanium photodetector [116] to a fundamental modification of the fingers of conventional metal–semiconductor-metal photodetectors (MSM-PDs) for SPP coupling [117]. To perform optimally, the MSM-PD must send as much energy as possible to the photodetectors interface. The total energy that can be harvested will be influenced by the geometry and optics of the structures, as well as the incident radiation characteristics (wavelength, polarization, angle of incidence, etc.).

When the wavelength of the light is in sync with the resonance of the particle, metal nanoparticles can have a powerful interaction with the light. The scattering direction and intensity, as well as the interaction strength and scattering cross-section, are all determined by the resonance frequency. The resonance frequency is affected by a wide variety of elements, such as the type of metal that is employed, the medium in which it is immersed, the size and form of the particles, and the photonic environment in which they are situated. The study of photovoltaics

Fig. 13 Different chip-scale device technologies' operating speeds [107]
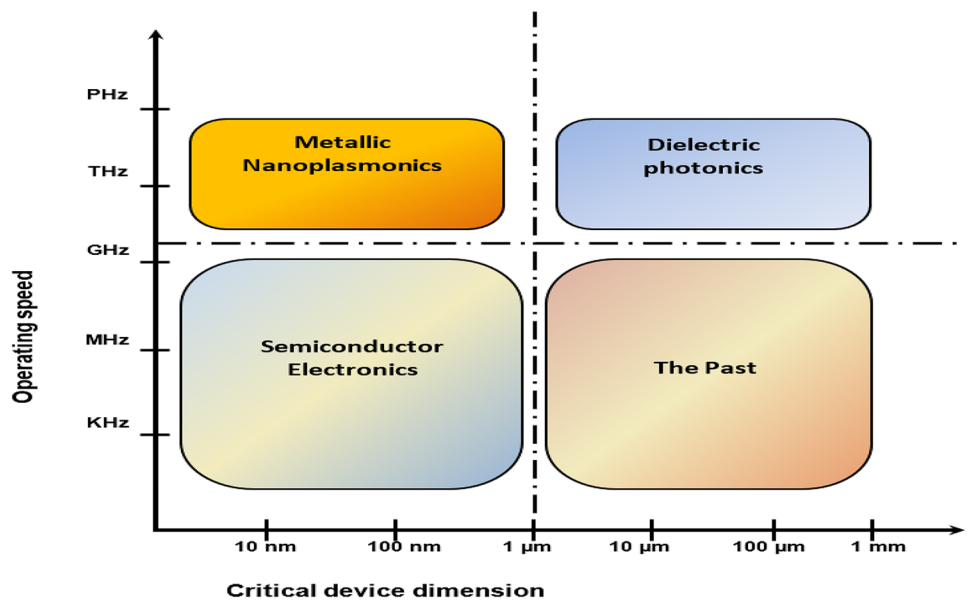
might be helped by three significant plasmonic processes in the future. When the wavelength of the light is in sync with the resonance of the particle, metal nanoparticles can have powerful interactions with the light, Fig. 15. The scattering direction and intensity, as well as the interaction strength and scattering cross-section, are all controlled by the resonance frequency. The resonance frequency is affected by a wide variety of parameters, such as the type of metal that was used, the medium in which it was immersed, the size and form of the particles, and the photonic environment in which the particles were situated. The study of photovoltaics could potentially gain from three significant plasmonic processes [118].

The first two theories are based on localized plasmon polaritons (LPPs), and they can give a local field enhancement to boost absorption near the particles. On
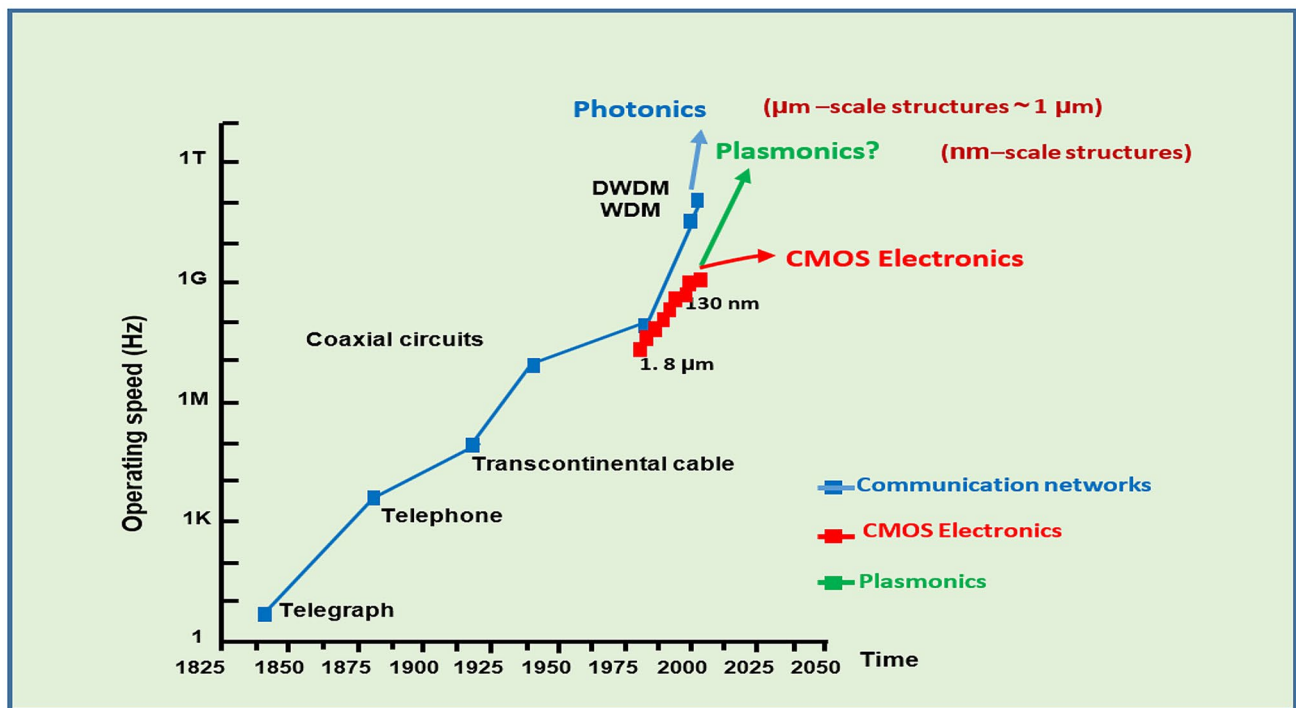
Fig. 14 The speed at which data transport and processing systems operate [108]

the other hand, the third idea depends on directional scattering and light trapping to increase absorption near the particles. The propagation of plasmons is the basis for the third and most recent mechanism that has been developed.

The directed scattering method is the most efficient of these procedures because it can be used to intentionally induce antireflection qualities if the light is dispersed into a high refractive index region. The problem with all of these systems is that the metal nanoparticles almost always cause parasitic absorption, which is a source of disagreement. Because parasitic absorption is especially effective at short wavelengths, depositing particles on the surface of a solar cell may reduce the cell's effectiveness. Aside from preventing short-wavelength parasitic losses, putting particles at the back of a cell allows the design to be specifically tailored to address large-angle scattering for the difficult near-band-edge photons that require light trapping [120]. However, progress has been slow, with only minor improvements in thin-film solar cell efficiencies revealed thus far [121]. The most promising approach is to be cautious when designing the shape, size, and distribution of metal nanoparticles in back reflector designs.

Silicon Thin-film Solar Cell Modeling

Single Solar Cell Modeling

The number of extracted parameters is used to classify compact (or non-numerical) models. PV approximations are classified into several types [122], Fig. 16. The one-diode model is widely accepted as an accurate representation of solar cells that achieves a reasonable balance of simplicity and accuracy. An attempt to improve that model is by including another diode or diodes and creating the "N-diode-based model." These approximations produce a set of unknown parameters, starting with two (the ideal approximation) and increasing to seven or more parameters [123].

Figure 17 depicts the block diagram for PV parameter extraction, with the main goal of solving the diode(s) equation using the given parameters, Eq. 1. Some parameters,

such as maximum power (Pm), open circuit voltage (Voc), and short circuit current (Jsc), can be obtained from PV manufacturing datasheets, while the rest, such as short circuit current and open circuit voltage variations due to light and temperature changes, can be extracted empirically, as shown in Eqs. 2 and 3. Consider the PV diode equation to begin.

$$I = I_o\left(e^{\frac{qV}{kT}} - 1\right) \tag{1}$$

where:

I_o: Dark current.
I: The net current flowing through the diode.
V: Applied voltage of the diode.
q: Absolute value of electron charge.
k: Boltzmann's constant.
T: Absolute temperature (K).

$$I_{sc} \propto (T, \gamma) \tag{2}$$

$$V_{oc} \propto (T, \gamma) \tag{3}$$

where T and γ are the ambient temperature and irradiation density, respectively. Please note that the electrons' or holes' temperature values are different from the temperature values used with those approximations, Eqs. (1–3). the temperature values used for the parameter extraction techniques are the ambient temperature, which is an incorrect definition and inconsistent with electron or hole transport. Of course, it can't be extracted using those approximations, and for this reason, an empirical parameter must be used to refine the results with those obtained numerically or experimentally.

Those models rely primarily on the PV diode (s) approximation equivalent circuits, which are then solved for circuit parameters such as photonic current (I_{ph}), series resistance (R_s), parallel resistance (R_p), ideality factor (n), junction capacitance (C_j), and so on.

To summarize, the parameters are solved inconsistently with the PV semiconductor, which is accepted with the definition of the compact models to reduce the time required for SPICE simulation calculations.

Fig. 15 Mechanisms for the plasmonic trapping of light for use in thin-film solar cells [119]
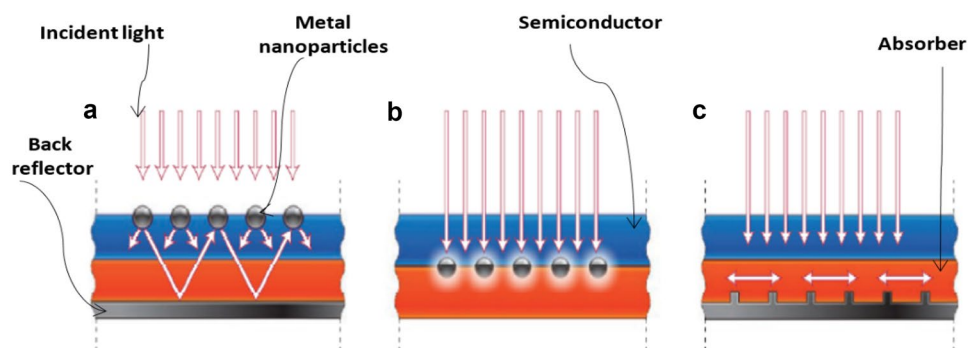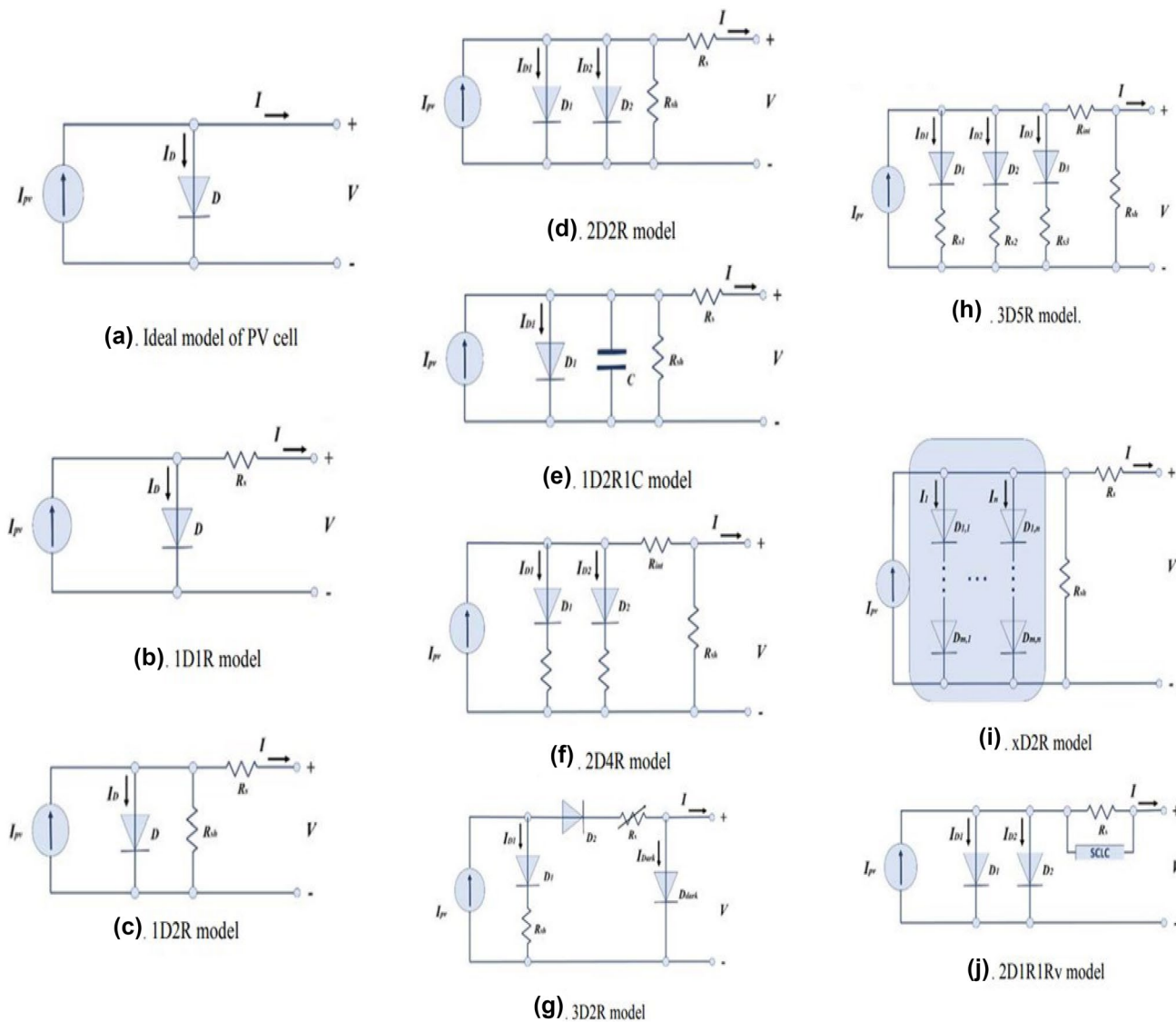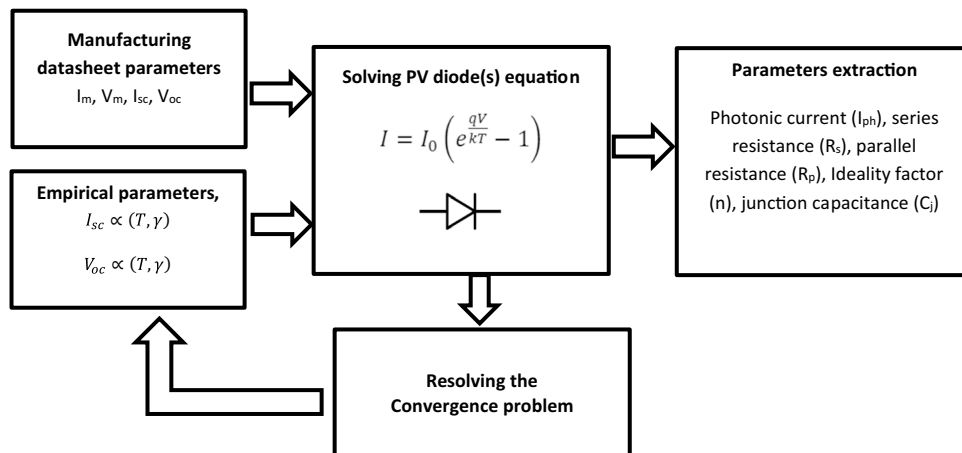
Fig. 16 different equivalent circuits of PV model approximations [122]

Fig. 17 Block diagram for PV parameters extraction

Array of Solar Cell Modeling

The introduced simulation for solar cells array as shown in Fig. 18, is based on the mathematical model, in which the PV module structure is created in SIMULINK/MATLAB to simulate thin-film solar cells. The main purpose of this part is to connect multi-physics modeling in COMSOL for single physical parameters to the entire array of a typical thin-film solar cell.

In this section, the complete array of thin-film solar cells is simulated using 26-rows by 264 columns (Ns x Np) as shown in Fig. 19 to study the effect of SPP on the efficiency depending on COMSOL Multiphysics parameters and the SIMULINK/MATLAB module [124].

Challenges, New Trends, and Future Work in Silicon Thin-film Solar Cell

Challenges in Silicon Thin-Film Solar Cell

Because it takes a significant amount of time to simulate a silicon thin-film solar cell, optimizing the performance of silicon thin-film solar cells using device simulation tools is difficult; however, PV-based compact models can save time. One solution is to use the equivalent circuit model in MATLAB to optimize the performance of a thin-film silicon solar cell.

New Trends

The following is a summary of the subjects that were deemed important:

A. **Topology Problem**

There are extensive studies in this area for many years. Studies are continually being conducted since an infinite number of topologies have yet to be uncovered. Until now, it has been impossible to find a single ideal topology that accounts for all of the necessary metrics.
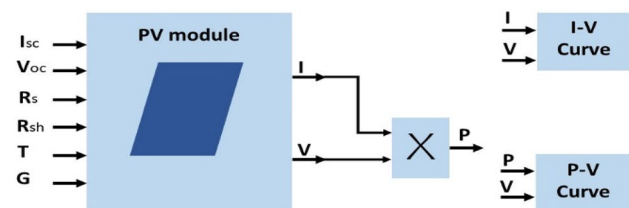

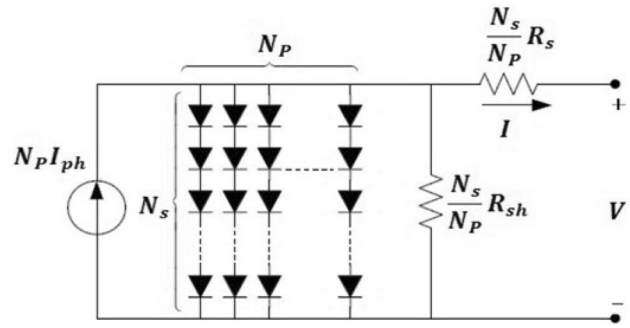**Fig. 18** PV module structure of the thin-film solar cell in SIMULINK/MATLAB

Fig. 19 array structure of the thin-film solar cell in SIMULINK/MATLAB [125]

B. **Thin Film Solar Cell Performance Under Different Environmental Conditions**

As numerous studies have shown, rising temperatures reduce the efficiency of solar cells due to recombination. The efficiency of solar cells is determined by analyzing their electrical properties, such as short-circuit current density (Jsc) and open-circuit voltage (Voc) [126]. The behavior of solar cells is studied at temperatures ranging from 15 (288 K) to 50 (323 K) and beyond [127].

C. **Thin Film Solar Cell Optimization Techniques For Simulation**

Surface grating is one of the light-trapping strategies that can be used to increase not only the photo-generated short-circuit current but also the open circuit voltage of a solar cell, according to published research. This is supported by the literature. As a result, the use of surface gratings in conjunction with IBSCs may be considered a viable option for reversing the decrease in Voc caused by the incorporation of QDs with a low effective bandgap into a solar cell's active material structure. Plasmonics, nanophotonics, and surface plasmons are also being researched.

Future Work

In this section, some future directions related to the silicon thin-film solar cell are still open issues and require further investigation such as:

1. Studying the possibility of fabrication.
2. Studying the possibility of using different optimization techniques to optimize the solar cell array.
3. Studying using parallel processing techniques to minimize the computing cost.

4. Using germanium instead of silicon and examining the efficiency improvement.
5. Apply more grating shapes with different dimensions.
6. Using different types of materials like copper and silver with SPPs.

Conclusion

This paper provides a comprehensive survey of silicon thin-film solar cells for the most important enabling technologies in the upcoming solar cell. We were able to demonstrate that a thin-film solar cell may be applied in a wide variety of different types of solar cell technologies. It is favored because it is economical, makes less use of material, and demonstrates a trend that is optimistically rising in terms of how effectively it works, and these are the reasons why it is favored. This research was conducted to provide a comprehensive analysis of silicon thin-film solar cells, beginning with their development to the most recent and cutting-edge laboratory-developed module. There is a review of the fantastic development of each technology, as well as its cell configuration, restrictions, equivalent circuit model, cell performance, and global market share. The available simulators and software packages have been shown. New advances in solar cells are also highlighted; these hold the potential to be significant variables and solutions in the process of the future's development. Because of this, we believe that a thin-film solar cell will play an increasingly important role in the manufacturing of solar cells in the years to come. Challenges, new trends, and open issues have been discussed. Finally, some future directions related to the silicon thin-film solar cell are discussed.

Availability of Data and Materials The datasets generated during and/or analyzed during the current study are available from the corresponding author upon reasonable request.

Declarations

Conflict of Interests The authors declare no competing interests.

Ethics approval 'Not applicable'.

Consent to Participate All the authors agreed to be involved in this research work.

Consent for Publication All the authors have been permitted to publish the results.

References

1. Kannan N, Vakeesan D (2016) Solar energy for future world review. Renew Sustain Energy Rev 62:1092–1105
2. Fahrenbruch AL, Bube RH (1983) Fundamentals of solar cells. London Academic Press Inc from Usenet
3. ElKhamisy KM, El-Rabaie S, Elagooz SS, Abd Elhamid H (2019) The effect of different surface grating shapes on thin film solar cell efficiency. 2019 International Conference on Innovative Trends in Computer Engineering (ITCE), pp 297–300
4. Yadav A, Kumar P, Rpsgoi M (2015) Enhancement in efficiency of PV cell through P&O algorithm. Int J Technol Res Eng 2:2642–2644
5. Mohammad Bagher A (2015) Types of solar cells and application. Am J Opt Photonics 3(5):94. https://doi.org/10.11648/j.ajop.20150305.17
6. ElKhamisy K, Abdelhamid H, Elagooz S, El-Rabaie E-S (2021) The effect of different surface plasmon polariton shapes on thin-film solar cell efficiency. J Comput Electron. https://doi.org/10.1007/s10825-021-01729-0
7. Atwater HA, Polman A (2010) A single-layer wide-angle negative-index metamaterial at visible frequencies. Nat Mater 9:407–412
8. Schuller JA, Barnard ES, Cai W, Jun YC, White JS, Brongersma ML (2010) Invit Rev Nat Mater 9:193–204
9. Gramotnev DK, Bozhevolnyi SI (2009) Nat Photonics 4:83 (2010)
10. Iqbal T et al (2019) An optimal Au grating structure for light absorption in amorphous silicon thin film solar cell. Plasmonics 14(1):147–154
11. Tabrizi AA, Pahlavan A (2020) Efficiency improvement of a silicon-based thin-film solar cell using plasmonic silver nanoparticles and an antireflective layer. Opt Commun 454
12. Yousif B, Abo-Elsoud MEA, Marouf H (2020) High-performance enhancement of a GaAs photodetector using a plasmonic grating. Plasmonics 15(5):1377–1387
13. Pahuja A, Parihar MS, Kumar D (2019) Performance enhancement of thin film solar cell using two-dimensional plasmonic grating in rear electrode. IEEE Trans Nanotechnol 18:626–634
14. Ishaque K, Salam Z (2011) A comprehensive MATLAB Simulink PV system simulator with partial shading capability based on two-diode model. Sol energy 85(9):2217–2227
15. Rasheed M, Alabdali O, Shihab S, Rashid T (2021) Evaluation and determination of the parameters of a photovoltaic cell by an iterative method. J Al-Qadisiyah Comput Sci Math 13(1):34

16. Abdelhamid H, El-Deib A, ElKhamisy K, El-Shekh K, Memon Z (2022) Experimental validation of different PV technologies using a physical-based model. Opt Quantum Electron 54(7):1–16

17. Stuckelberger M, Biron R, Wyrsch N, Haug F-J, Ballif C (2017) Progress in solar cells from hydrogenated amorphous silicon. Renew Sustain Energy Rev 76:1497–1523

18. Lee TD, Ebong AU (2017) A review of thin film solar cell technologies and challenges. Renew Sustain Energy Rev 70:1286–1297

19. Kowsar A et al (2019) Progress in major thin-film solar cells: Growth technologies, layer materials, and efficiencies. Int J Renew Energy Res 9(2):579–597

20. Efaz ET, Ava AA, Khan MDTA, Islam MDM, Sultana A (2016) Parametric Analysis of CdTe/CdS Thin Film Solar Cell. Int J Adv Res Comput Commun Eng 5(6):401–404

21. Sai H, Matsui T, Matsubara K (2016) Stabilized 14.0%-efficient triple-junction thin-film silicon solar cell. Appl Phys Lett 109(18):183506

22. Hegedus S, Luque A (2003) Handbook of photovoltaic science and engineering

23. Schuettauf J-W et al (2015) Amorphous silicon–germanium for triple and quadruple junction thin-film silicon-based solar cells. Sol Energy Mater Sol Cells 133:163–169

24. Tanimoto H, Arai H, Mizubayashi H, Yamanaka M, Sakata I (2014) Light-induced hydrogen evolution from hydrogenated amorphous silicon: Hydrogen diffusion by formation of bond centered hydrogen. J Appl Phys 115(7):73503

25. Choubey PC, Oudhia A, Dewangan R (2012) A review: solar cell current scenario and future trends. Recent Res Sci Technol 4(8):99–101

26. Xing Y et al (2015) A review of concentrator silicon solar cells. Renew Sustain Energy Rev 51:1697–1708

27. Badawy WA (2015) A review on solar cells from Si-single crystals to porous materials and quantum dots. J Adv Res 6(2):123–132

28. Chopra KL, Paulson PD, Dutta V (2004) Thin-film solar cells: an overview. Prog Photovoltaics Res Appl 12(2–3):69–92

29. Sichanugrist P, Suzuki H, Konagai M, Takahashi K (1986) High-rate preparation of amorphous-silicon solar cells with monosilane. Jpn J Appl Phys 25(3R):440

30. Shah A, Torres P, Tscharner R, Wyrsch N, Keppner H (1999) Photovoltaic technology: the case for thin-film solar cells. Science 285(5428):692–698

31. Lee TD, Ebong A (2015) Thin film solar technologies: a review. 2015 12th International Conference on High-capacity Optical Networks and Enabling/Emerging Technologies (HONET), pp 1–10

32. Bertolli M (2008) Solar cell materials. Course: Solid State II. Dep. Physics, Univ. Tennessee, Knoxv, Knoxv

33. Makrides G, Zinsser B, Norton M, Georghiou GE (2012) Performance of photovoltaics under actual operating conditions. Third generation photovoltaics. Intechopen

34. Jayakumar P (2009) Solar energy resource assessment handbook, Asian and Pacific Centre for Transfer of Technology (APCTT) of the United Nations. ESCAP

35. Würfel P, Würfel U (2016) Physics of solar cells: from basic principles to advanced concepts. John Wiley & Sons

36. Dubey S, Sarvaiya JN, Seshadri B (2013) Temperature-dependent photovoltaic (PV) efficiency and its effect on PV production in the world–a review. Energy Procedia 33:311–321

37. Ghahremani A, Fathy AE (2015) A three-dimensional multiphysics modeling of thin-film amorphous silicon solar cells. Energy Sci Eng 3(6):520–534

38. Yousif B, Abo-Elsoud MEA, Marouf H (2019) Triangle grating for enhancement the efficiency in thin film photovoltaic solar cells. Opt Quantum Electron 51(8):276. https://doi.org/10.1007/s11082-019-1987-5

39. Zia R, Saleemi F, Naseem S, Kayani Z (2015) Study the efficiency of single crystal CdTe/ZnCdS solar cell at various temperatures and illumination levels. Energy Rep 1:58–61

40. Srinivas B, Balaji S, Nagendra Babu M, Reddy YS (2015) Review on present and advance materials for solar cells. Int J Eng Res 3:178–182

41. Razykov TM, Ferekides CS, Morel D, Stefanakos E, Ullal HS, Upadhyaya HM (2011) Solar photovoltaic electricity: Current status and future prospects. Sol energy 85(8):1580–1608

42. Troshin PA et al (2009) Material solubility-photovoltaic performance relationship in the design of novel fullerene derivatives for bulk heterojunction solar cells. Adv Funct Mater 19(5):779–788

43. Brabec CJ, Shaheen SE, Winder C, Sariciftci NS, Denk P (2002) Effect of LiF/metal electrodes on the performance of plastic solar cells. Appl Phys Lett 80(7):1288–1290

44. Suhaimi S, Shahimin MM, Alahmed ZA, Chyský J, Reshak AH (2015) Materials for enhanced dye-sensitized solar cell performance: Electrochemical application. Int J Electrochem Sci 10(4):2859–2871

45. Graetzel M, Janssen RAJ, Mitzi DB, Sargent EH (2012) Materials interface engineering for solution-processed photovoltaics. Nature 488(7411):304–312

46. Sharma S, Jain KK, Sharma A (2015) Solar cells: in research and applications- a review. Mater Sci Appl 6(12):1145

47. Wernick MN, Aarsvold JN (2004) Emission tomography: the fundamentals of PET and SPECT. Elsevier (ISBN 0-12-744482-3 (alk. paper) 1. Tomography, Emission. I. Wernick, Miles. II. Aarsvold, John. [DNLM: 1. Tomography, Emission-Computed. 2. Tomography, Emission-Computed, Single-Photon. WN 206 E53 2004] RC78.7.T62E455 2004 616.07'575–dc22)

48. Carlson DE, Wronski CR (1976) Amorphous silicon solar cell. Appl Phys Lett 28(11):671–673

49. Carlson DE, Wronski CR (1977) Solar cells using discharge-produced amorphous silicon. J Electron Mater 6(2):95–106

50. Carlson DE (1980) Recent developments in amorphous silicon solar cells. Sol Energy Mater 3(4):503–518

51. Tawada Y, Kondo M, Okamoto H, Hamakawa Y (1982) Hydrogenated amorphous silicon carbide as a window material for high efficiency a-Si solar cells. Sol Energy Mater 6(3):299–315

52. Yablonovitch E, Cody GD (1982) Intensity enhancement in textured optical sheets for solar cells. IEEE Trans Electron Devices 29(2):300–305

53. Yamazaki S et al (1986) Fabrication of the large-area integrated a-Si solar cells, vol 70. MRS Online Proc Libr

54. Guha S, Yang J, Banerjee A, Glatfelter T, Xu X (1992) Advances in amorphous silicon alloy-based multijunction cells and modules. AIP Conf Proc 268(1):64–71

55. Yang J, Banerjee A, Guha S (1997) Triple-junction amorphous silicon alloy solar cell with 14.6% initial and 13.0% stable conversion efficiencies. Appl Phys Lett 70(22):2975–2977

56. Sai H et al (2015) Triple-junction thin-film silicon solar cell fabricated on periodically textured substrate with a stabilized efficiency of 13.6%. Appl Phys Lett 106(21):213902

57. Kazmerski LL, White FR, Morgan GK (1976) Thin-film CuInSe2/CdS heterojunction solar cells. Appl Phys Lett 29(4):268–270

58. Grindle SP, Clark AH, Rezaie-Serej S, Falconer E, McNeily J, Kazmerski LL (1980) Growth of CuInSe2 by molecular beam epitaxy. J Appl Phys 51(10):5464–5469

59. Chen WS, Mickelsen RA (1980) Thin-film CdS/CuInSe2 heterojunction solar cell. Role of electro-optics in photovoltaic energy conversion 248:62–69

60. Mickelsen RA, Chen WS (1981) Development of a 9.4% efficient thin-film CuInSe2/CdS solar cell. 15th photovoltaic specialists conference, pp 800–804

61. Mickelsen RA, Chen WS (1982) Polycrystalline thin-film CuInSe/sub 2/solar cells. Conf Rec IEEE Photovoltaic Spec Conf, United States (no. CONF-820906)

62. Potter RR, Eberspacher C, Fabick LB (1985) Device analysis of CuInSe2/(Cd, Zn) S/ZnO solar cells. Photovoltaic Specialists Conference, pp 1659–1664

63. Mitchell KW, Liu HI (1996) Device analysis of CuInSe/sub 2/ solar cells. Conference Record of the Twentieth IEEE Photovoltaic Specialists Conference, pp 1461–1468

64. Devaney WE, Chen WS, Stewart JM, Mickelsen RA (1990) Structure and properties of high-efficiency ZnO/CdZnS/CuInGaSe/sub 2/solar cells. IEEE Trans Electron Devices 37(2):428–433

65. Gabor AM, Tuttle JR, Albin DS, Contreras MA, Noufi R, Hermann AM (1994) High-efficiency CuIn x Ga1− x Se2 solar cells made from (In x, Ga1− x) 2Se3 precursor films. Appl Phys Lett 65(2):198–200

66. Ramanathan K et al (1996) Effect of heat treatments and window layer processing on the characteristics of CuInGaSe/sub 2/thin film solar cells. Conference Record of the Twenty-Fifth IEEE Photovoltaic Specialists Conference-1996, pp 837–840

67. Contreras MA et al (1999) Progress toward 20% efficiency in Cu (In, Ga) Se2 polycrystalline thin-film solar cells. Prog Photovoltaics Res Appl 7(4):311–316

68. Ramanathan K et al (2003) Properties of 19.2% efficiency ZnO/CdS/CuInGaSe2 thin-film solar cells. Prog Photovoltaics Res Appl 11(4):225–230

69. Contreras MA et al (2005) ACCELERATED PUBLICATION: Diode characteristics in state-of-the-art ZnO/CdS/Cu (In1− xGax) Se2 solar cells. Prog photovoltaics Res Appl 13(3):209–216

70. Repins I et al (2008) 19· 9%-efficient ZnO/CdS/CuInGaSe2 solar cell with 81· 2% fill factor. Prog Photovoltaics Res Appl 16(3):235–239

71. Jackson P et al (2011) New world record efficiency for Cu (In, Ga) Se2 thin-film solar cells beyond 20%. Prog Photovoltaics Res Appl 19(7):894–897

72. Hall M (2013) EMPA announces 20.4% efficient thin-film CIGS-on-polymer cell, vol 21. PV Mag

73. Powalla M et al (2013) High-efficiency cu (in, ga) se2 cells and modules. Sol Energy Mater Sol Cells 119:51–58

74. Jackson P, Hariskos D, Wuerz R, Wischmann W, Powalla M (2014) Compositional investigation of potassium doped Cu (In, Ga) Se2 solar cells with efficiencies up to 20.8%. Phys status solidi (RRL)–Rapid Res Lett 8(3):219–222

75. Herrmann D et al (2014) CIGS module manufacturing with high deposition rates and efficiencies. 2014 IEEE 40th Photovoltaic Specialist Conference (PVSC), pp 2775–2777

76. Jackson P et al (2015) Properties of Cu (In, Ga) Se2 solar cells with new record efficiencies up to 21.7%. Phys Status Solidi (RRL)–Rapid Res Lett 9(1):28–31

77. Rudmann D et al (2004) Efficiency enhancement of Cu (In, Ga) Se 2 solar cells due to post-deposition Na incorporation. Appl Phys Lett 84(7):1129–1131

78. Gifford J (2015) Solar frontier hits 22.3% on CIGS cell. pv Mag

79. Pässler R (1999) Parameter sets due to fittings of the temperature dependencies of fundamental bandgaps in semiconductors. Phys status solidi 216(2):975–1007

80. Nakayama N, Matsumoto H, Yamaguchi K, Ikegami S, Hioki Y (1976) Ceramic thin film CdTe solar cell. Jpn J Appl Phys 15(11):2281

81. Mitchell KW, Fahrenbruch AL, Bube RH (1977) Evaluation of the CdS/CdTe heterojunction solar cell. J Appl Phys 48(10):4365–4371

82. Tyan Y-S (1982) Semiconductor devices having improved low-resistance contacts to p-type CdTe, and method of preparation. Google Patents Mar. 09

83. Tyan Y-S, Perez-Alburne EA (1982) Efficient thin-film CdS/CdTe solar cells. Conf Rec IEEE Photovoltaic Spec Conf, United States (no. CONF-820906-)

84. Werthen JG, Fahrenbruch AL, Bube RH, Zesch JC (1983) Surface preparation effects on efficient indium-tin-oxide-CdTe and CdS-CdTe heterojunction solar cells. J Appl Phys 54(5):2750–2756

85. Kuribayashi K, Matsumoto H, Uda H, Komatsu Y, Nakano A, Ikegami S (1983) Preparation of low resistance contact electrode in screen printed CdS/CdTe solar cell. Jpn J Appl Phys 22(12R):1828

86. Meyers PV (1988) Design of a thin film CdTe solar cell. Sol cells 23(1–2):59–67

87. Mitchell KW, Eberspacher C, Cohen F, Avery J, Duran G, Bottenberg W (1988) Progress towards high-efficiency thin-film CdTe solar cells. Sol cells 23(1–2):49–57

88. Albright SP, Jordan JF, Ackerman B, Chamberlin RR (1989) Developments on CdS/CdTe photovoltaic panels at photon energy, inc. Sol Cells 27(1–4):77–90

89. Morris GC, Tanner PG, Tottszer A (1990) Towards high-efficiency electrodeposited CdS/CdTe thin film cells. IEEE Conf Photovoltaic Specialists, pp 575–580

90. Chu TL, Chu SS, Ferekides C, Wu CQ, Britt J, Wang C (1991) 13.4% efficient thin-film CdS/CdTe solar cells. J Appl Phys 70(12):7608–7612

91. Chu TL et al (1992) 14.6% efficient thin-film cadmium telluride heterojunction solar cells. IEEE electron device Lett 13(5):303–304

92. Ferekides CS, Britt J, Ma Y, Killian L (1993) High-efficiency CdTe solar cells by close spaced sublimation. Conference Record of the Twenty Third IEEE Photovoltaic Specialists Conference (Cat. No. 93CH3283–9), pp 389–393

93. Shockley W, Queisser HJ (1961) Detailed balance limit of efficiency of p-n junction solar cells. J Appl Phys 32(3):510–519

94. Islam A, Das A, Sarkar N, Matin MA, Amin N (2018) Numerical analysis of PbSe/GaAs quantum dot intermediate band solar cell (QDIBSC). 2018 International Conference on Computer, Communication, Chemical, Material and Electronic Engineering (IC4ME2), pp 1–6

95. Luque A, Martí A (1997) Increasing the efficiency of ideal solar cells by photon induced transitions at intermediate levels. Phys Rev Lett 78(26):5014

96. Bucik R et al (2021) The long period of 3He-rich solar energetic particles measured by Solar Orbiter 2020 November 17–23. Energy (MeV/nuc) 10(1):100

97. Luque A, Martí A, Stanley C (2012) Understanding intermediate-band solar cells. Nat Photonics 6(3):146–152

98. Zhu M et al (2019) Efficient PbSe colloidal quantum dot solar cells using SnO2 as a buffer layer. ACS Appl Mater Interfaces 12(2):2566–2571

99. Aly AE-MM, Nasr A (2016) Theoretical comparative study of quantum dot solar cell behavior for single and multi-intermediate bands. J Energy Eng 142(4):4016007

100. Imran A et al (2018) Efficiency enhancement through flat intermediate band in Quantum dot solar cell. Results Phys 10:241–247

101. Okada Y et al (2015) Intermediate band solar cells: Recent progress and future directions. Appl Phys Rev 2(2):21302

102. Chang WC, Yang MJ, Yarn KF, Chuang WC (2012) Analyses of one-dimensional gratings on the performance of solar cells. J Ovonic Res 8(2):53–64

103. Elewa S, Yousif B, Abo-Elsoud MEA (2021) Efficiency enhancement of intermediate band solar cell using front surface pyramid grating. Opt Quantum Electron 53(7):1–18

104. Muhammad MH, Hameed MFO, Obayya SSA (2017) Broadband absorption enhancement in modified grating thin-film solar cell. IEEE Photonics J 9(3):1–14

105. Lee HC, Lee W, Moon JH, Kim D (2019) Geometric effect of grating-patterned electrode for high conversion efficiency of dye-sensitized solar cells. Multiscale Sci Eng 1(2):161–166

106. Ding F, Wang Z, He S, Shalaev VM, Kildishev AV (2015) Broadband high-efficiency half-wave plate: a supercell-based plasmonic metasurface approach. ACS Nano 9(4):4111–4119

107. Brongersma ML, Shalaev VM (2010) The case for plasmonics. Science 328(5977):440–441

108. Viaene S, Ginis V, Danckaert J, Tassin P (2017) Mitigating optical singularities in coordinate-based metamaterial waveguides. Phys Rev B 95(15)

109. Ozbay E (2006) Plasmonics: merging photonics and electronics at nanoscale dimensions. Science 311(5758):189–193

110. Atwater HA (2007) The promise of plasmonics. Sci Am 296(4):56–63

111. Maier SA (2007) Plasmonics: fundamentals and applications, vol 1. Springer

112. Zia R, Schuller JA, Chandran A, Brongersma ML (2006) Plasmonics: the next chip-scale technology. Mater today 9(7–8):20–27

113. Xie Z et al (2011) Plasmonic nanolithography: a review. Plasmonics 6(3):565–580

114. Schuller JA, Barnard ES, Cai W, Jun YC, White JS, Brongersma ML (2010) Plasmonics for extreme light concentration and manipulation. Nat Mater 9(3):193–204

115. Kashyap R, Nemova G (2009) Surface plasmon resonance-based fiber and planar waveguide sensors. J Sensors 2009:645162

116. Tang L et al (2006) C-shaped nanoaperture-enhanced germanium photodetector. Opt Lett 31(10):1519–1521

117. Ren F-F et al (2010) Surface plasmon enhanced responsivity in a waveguided germanium metal-semiconductor-metal photodetector. Appl Phys Lett 97(9):91102

118. Atwater HA, Polman A (2011) Plasmonics for improved photovoltaic devices. Mater. Sustain. energy a Collect. peer-reviewed Res. Rev. Artic. from Nat. Publ. Gr., pp 1–11

119. Juan ML, Righini M, Quidant R (2011) Plasmon nano-optical tweezers. Nat Photonics 5(6):349–356

120. Temple TL, Mahanama GDK, Reehal HS, Bagnall DM (2009) Influence of localized surface plasmon excitation in silver nanoparticles on the performance of silicon solar cells. Sol Energy Mater Sol Cells 93(11):1978–1985

121. Yin Y et al (2017) Topology induced anomalous plasmon modes in metallic Möbius nanorings. Laser Photon Rev 11(2):1600219

122. Abbassi R, Abbassi A, Jemli M, Chebbi S (2018) Identification of unknown parameters of solar cell models: a comprehensive overview of available approaches. Renew Sust Energy Rev 90:453–474. https://doi.org/10.1016/j.rser.2018.03.011

123. Nassar-Eddine I, Obbadi A, Errami Y, Agunaou M (2016) Parameter estimation of photovoltaic modules using iterative method and the Lambert W function: A comparative study. Energy Convers Manag 119:37–48

124. ElKhamisy K, Abdelhamid H, Elagooz S, El-Rabaie E-SM (2021) The effects of surface plasmon polariton on silicon thin film solar cell array. 2021 9th International Japan-Africa Conference on Electronics, Communications, and Computations (JAC-ECC), pp 65–68

125. Abdullah FS, Hamoodi SA, Hamoodi AN (2018) Modeling of electrical characteristics of photo voltaic and effecting of cell parameters on V-I curve. Int J Eng Technol 7(2.13):276–280. https://doi.org/10.14419/ijet.v7i2.13.12680

126. Contreras MA, Nakada T, Hongo M, Pudov AO, Sites JR (2003) Zno/zns (o, oh)/cu (in, ga) se/sub 2//mo solar cell with 18.6% efficiency, vol 1. Proceedings of 3rd World Conference on Photovoltaic Energy Conversion, pp 570–573

127. Sze SM, Li Y, Ng KK (2021) Physics of semiconductor devices. John Wiley & Sons